March, 1988] © 1988 The Chemical Society of Japan Bull. Chem. Soc. Jpn., 61, 945—951 (1988) 945

Solvation Structure of Copper(II) Ion in *N,N*-Dimethylformamide and *N,N*-Dimethylformamide–Acetonitrile Mixtures Determined by the X-Ray Diffraction Method

Kazuhiko Ozutsumi, Shin-ichi Ishiguro,* and Hitoshi Ohtaki[†]
Coordination Chemistry Laboratories, Institute for Molecular Science, Myodaiji, Okazaki 444
[†]Department of Electronic Chemistry, Tokyo Institute of Technology at Nagatsuta,
Nagatsuta-cho 4259, Midori-ku, Yokohama 227

(Received September 14, 1987)

The solvation structure of copper(II) ion in *N,N*-dimethylformamide (DMF) and *N,N*-dimethylformamide–acetonitrile (AN) mixtures has been investigated by means of X-ray diffraction at 25 °C. The X-ray scattering data for the copper(II) perchlorate DMF solution were well-interpreted in terms of the presence of the axially elongated octahedral $[Cu(dmf)_6]^{2+}$ ion in DMF. Among the six DMF molecules, four of them are at the distance of 203(3) pm at the equatorial position and the other two are at 243(5) pm at the axial one. On the other hand, in copper(II) perchlorate DMF–AN solutions with the C_{dmf}/C_{Cu} mole ratios of 5.308 and 7.435, where C_i denotes the total concentrations of species *i*, the copper(II) ion is coordinated with four DMF molecules within the square-plane and with no solvent molecule along the axis of the plane. The equatorial Cu–O bond length is 200(1) pm and practically the same as that within the $[Cu(dmf)_6]^{2+}$ ion in DMF. In copper(II) nitrate DMF solutions (1.086 and 1.500 mol dm^{-3}), a nitrate ion binds to copper(II) ion at the equatoral position and the distorted octahedral $[CuNO_3(dmf)_5]^+$ complex is formed.

Complex formation reactions between copper(II) and chloride ions in *N,N*-dimethylformamide (DMF) and in acetonitrile (AN) have been investigated[1,2] and it was found that the formation of copper(II)–chloro complexes ($[CuCl_n]^{(2-n)+}$, $n=1$—4) is more favorable in AN than in DMF. The more enhanced formation of the complexes in AN than in DMF is mainly ascribed to the difference in the donor property between the two solvents, i.e. copper(II) ion is more strongly solvated with DMF than with AN. Accordingly, copper(II) ion is preferentially solvated with DMF molecules in DMF–AN mixtures[3] and complex formation between copper(II) and chloride ions in the mixtures depends on the solvent composition.[4]

According to the X-ray diffraction study, copper(II) ion in aqueous solution is coordinated with six water molecules and the $[Cu(H_2O)_6]^{2+}$ ion has an axially elongated octahedral structure.[5] However, structural information on solvated copper(II) ion in other solvents has never been given by the diffraction method. In the present study we aimed at determining the solvation structure of copper(II) ion in DMF and in DMF–AN mixtures by the X-ray diffraction method. It was difficult to determine the solvation structure of copper(II) ion in AN because of a low solubility of copper(II) perchlorate in AN.

Experimental

Preparation of Sample Solutions. All chemicals used were of reagent grade. *Copper(II) perchlorate DMF solvate* was prepared by dissolving copper(II) perchlorate hydrate crystals in DMF and by repeated evaporation of DMF to remove water, and was finally isolated by adding ether. Crude crystals thus obtained were recrystallized from a DMF–acetone mixture. *Copper(II) nitrate DMF solvate* was obtained by a similar way to that used for copper(II) pechlorate DMF solvate and then recrystallized from DMF. Crystals thus obtained were dried at 40 °C in a vaccum oven for several days and stored in a vaccum desiccator over P_2O_5. From the electrogravimetric analysis of copper, the composition of the solvate crystals prepared was found to be $Cu(ClO_4)_2(dmf)_4$ and $Cu(NO_3)_2(dmf)_2$. *N,N*-Dimethyformamide and acetonitrile were purified by similar ways to those described in previous papers.[1,2]

Five test solutions A to E were prepared for X-ray diffraction measurements as shown in Table 1. Solution A was prepared by dissolving the copper(II) perchlorate DMF solv-

Table 1. The Composition (mol dm^{-3}), Stoichiometric Volumes V per Copper Atom and Densities ρ of the Sample Solutions

	A	B	C	D	E
Cu^{2+}	0.5513	1.086	1.500	0.9388	0.8856
ClO_4^-	1.103	—	—	1.878	1.771
NO_3^-	—	2.172	3.000	—	—
DMF	12.54	12.28	11.99	4.983	6.584
AN	—	—	—	10.83	8.510
$V/10^9$ pm^3	3.012	1.592	1.107	1.769	1.875
ρ/g cm^{-3}	1.061	1.101	1.158	1.055	1.063
$C_{dmf}/C_{Cu^{2+}}$	22.75	11.31	7.993	5.308	7.435

ate in DMF and was an almost saturated one at room temperature. Solutions B and C are copper(II) nitrate DMF solution in which the concentration of copper(II) ions is higher than that in solution A. Solutions D and E are copper(II) perchlorate solutions in DMF-AN mixtures of different molar ratios. Concentrations of copper(II) ions in the test solutions were determined by electrogravimetry. Concentrations of perchlorate and nitrate ions in the solutions were estimated from the stoichiometry of the copper(II) salts used. Densities of the sample solutions were measured by using a pycnometer.

X-Ray Scattering Measurements. X-Ray scattering measurements were carried out with a θ-θ type diffractometer (JEOL DX-GO-Y) by using an Mo X-ray tube (λ=71.07 pm). Scattered X-rays were monochromatized by a Johansson-type graphite monochromator and a pulse-height analyzer. The observed range of the scattering angle 2θ was from 2° to 140° and times required to collect 240000 counts at each angle were recorded. Corrections for the scattered intensities were made by the same manner as that described elsewhere.(6)

The reduced intensities $i(s)$ were obtained by subtracting independent coherent scatterings from the measured intensities $I(s)$ as follows:

$$i(s) = K\cdot I(s) - \sum_i \mathrm{n}_i[\{f_i(s) + \Delta f_i'\}^2 + (\Delta f_i'')^2], \tag{1}$$

where K stands for a normalization factor of the measured intensities to the absolute ones. n_i is the number of atom i in a stoichiometric volume V per copper atom of the test solutions. $f_i(s)$ represents the atomic scattering factors at s, and $\Delta f_i'$ and $\Delta f_i''$ denote the real and imaginary parts of anomolous dispersion, respectively, of atom i. The reduced intensities multiplied by s $(=4\pi\lambda^{-1}\sin\theta)$ for the sample solutions are shown in Fig. 1.

The radial distribution function $D(r)$ was calculated by the Fourier transform of the reduced intensities according to Eq. 2:

$$D(r) = 4\pi r^2\rho_0 + \frac{2r}{\pi}\int_0^{s_{\max}} s\cdot i(s)\cdot M(s)\cdot\sin(rs)\mathrm{d}s, \tag{2}$$

where ρ_0 $(=\{\sum \mathrm{n}_i\cdot f_i(0)\}^2/V)$ is the average scattering density in a stoichiometric volume of the sample solution and $s_{\max}$ represents the maximum s-value attained in the measurement ($s_{\max}$=16.6×10^{-2} pm^{-1}). The modification function $M(s)$ is given as

$$M(s) = \frac{\sum_i \mathrm{n}_i\{(f_i(0) + \Delta f_i')^2 + (\Delta f_i'')^2\}}{\sum_i \mathrm{n}_i\{(f_i(s) + \Delta f_i')^2 + (\Delta f_i'')^2\}}\cdot\exp(-ks^2). \tag{3}$$

The damping factor k was chosen as 100 pm^2 in the present case. The differential radial distribution curves, $D(r)-4\pi r^2\rho_0$, for the test solutions are depicted in Fig. 2.

A least-squares calculation for the refinement of the structure parameters was applied to the reduced intensities so as to minimize the error-square sum U,

$$U = \sum_{s_{\max}}^{s_{\max}} s^2\{i(s)_{\mathrm{obsd}} - i(s)_{\mathrm{calcd}}\}^2. \tag{4}$$

The theoretical intensities $i(s)_{\mathrm{calcd}}$ arising from the inter-

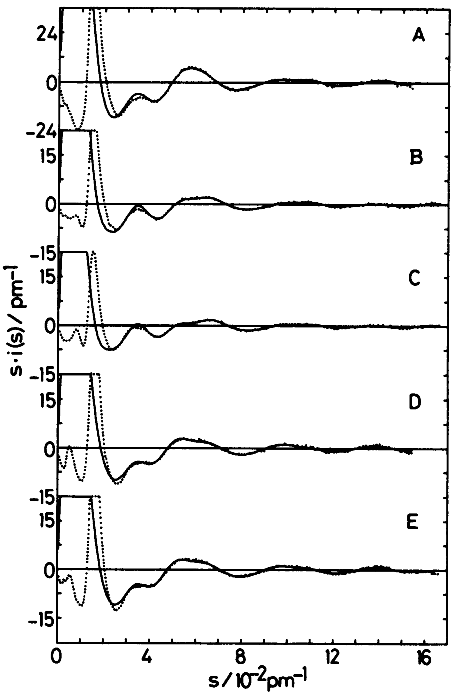

Fig. 1. The reduced intensities multiplied by s for solutions A to E. The observed $s\cdot i(s)$ values are shown by the dotted lines and calculated ones by the solid lines.

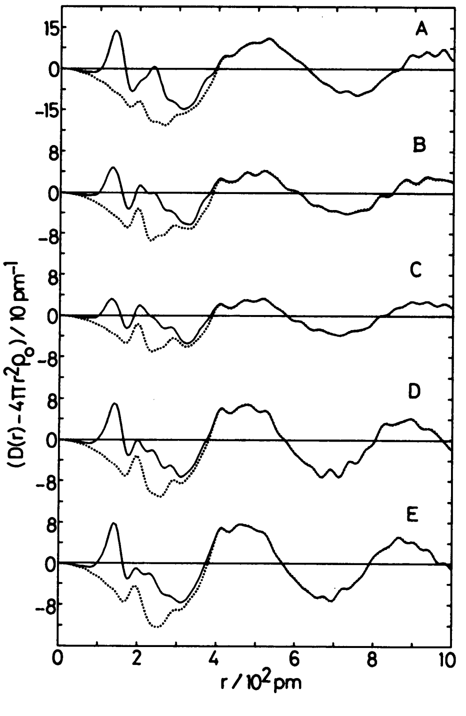

Fig. 2. The differential radial distribution curves, $(D(r)-4\pi r^2\rho_0)$, for solutions A to E. The dotted lines indicate the residual curves after subtraction of peaks due to intramolecular interactions of solvent molecules and anions.

atomic interactions in the solutions are obtained as follows:

$$i(s)_{\mathrm{calcd}}=\sum_{i}\sum_{\substack{j\\ i\neq j}} n_{ij}[\{f_i(s)+\Delta f_i'\}\{f_j(s)+\Delta f_j'\}+(\Delta f_i'')(\Delta f_j'')] \cdot \frac{\sin(r_{ij}s)}{r_{ij}s}\cdot \exp(-b_{ij}s^2), \quad (5)$$

where r_{ij}, b_{ij}, and n_{ij} represent the distance, the temperature factor, and the frequency factor of the atom-pair i–j, respectively.

All calculations were performed by using programs KURVLR[7] and NLPLSQ.[8]

Results and Discussion

The observed $(D(r)-4\pi r^2\rho_o)$ curves for solutions A to E drawn by the solid lines in Fig. 2 show five peaks around 140, 200, 240, 290, and 400 pm in the range of $r\leqslant 400$ pm. Two large peaks are observed around 400—600 and 800—1000 pm, which are due to ion-ion, ion-solvent, and solvent-solvent long range intermolecular interactions, and they, except for the small peak at 400 pm, are not analyzed in the present study. Diffraction studies on the structure of liquid DMF[9] and AN[10,11] showed that the peaks resulting from the intramolecular interactions within solvent molecules appeared at 130 and 230 pm for DMF and 130 and 260 pm for AN. The first peak at 140 pm, therefore, consists of peaks due to C–H, C=O, and C–N bonds within DMF molecules in solutions A to E and due to C–H, C–C, and C≡N bonds within AN molecules in solutions D and E. The Cl–O bonds within perchlorate ions in solutions A, D and E, and the N–O bonds within nitrate ions in solutions B and C also contribute to the peak. The third peak appearing at 240 pm is due to the nonbonding N···O, C···C, and C···O interactions within DMF molecules and the C···N interactions within AN molecules. The O···O contacts within perchlorate and nitrate ions are partly contained in the peak.

In order to extract peaks due to the sole intramolecular interactions within solvated copper(II) ion, the calculated peak shapes due to the intramolecular interactions of solvent molecules and anions must be subtracted from the observed radial distribution functions. For the calculation the structural parameters of each solvent molecule were assumed to be the same as those reported in the liquid state.[9–11] The parameter values of perchlorate and nitrate ions were also taken from the literature.[5,12]

The dotted lines in Fig. 2 represent the residual radial distribution curves after subtracting the theoretical peak shapes due to the intramolecular interactions of solvent molecules and anions, and the curve shows the peaks originating from the intramolecular interactions within the solvated copper(II) ion over the region $r<400$ pm. The structure parameters of the solvated copper(II) ions in DMF and in DMF–AN mixtures, details of which will be discussed in the following sections, were evaluated by analyzing the residual curves.

Copper(II) Perchlorate DMF Solution. Figure 3a depicts the $(D(r)-4\pi r^2\rho_o)$ curve of solution A. Subtraction of the calculated peak shapes due to the intramolecular structure of DMF molecule and perchlorate ion from the original curve (solid line) gives the residual curve (chain line), which shows three peaks at 200, 290, and 400 pm and a small hump at 240 pm. The peak centered at 200 pm is ascribable to the Cu–O(dmf) bonds similar to the Cu–O(H_2O) within the hexaaquacopper(II) ion.[5] The area under the peak gives the frequency factor of four for the Cu–O bond. The peak at 290 pm is attributable to the nonbonding Cu···C interactions when the DMF molecules at the equatorial position direct lone-pair electrons of the oxygen atom to the central copper(II) ion as found in $SbCl_5$·DMF solvate crystal.[13] The nonbonding interligand O(eq)···O(eq) interactions might also be contained in the peak. If the structure of DMF molecules within the metal solvate is the same as that in the liquid state,[9] it is expected that the nonbonding Cu···N(eq) distance should

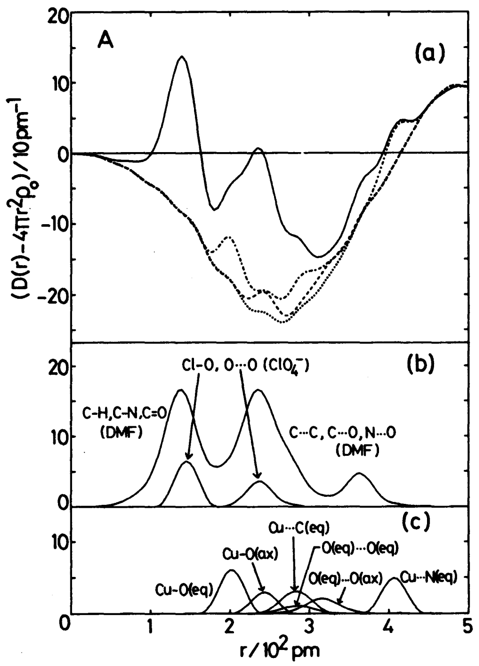

Fig. 3. (a); The $(D(r)-4\pi r^2\rho_o)$ curve for solution A. The chain line represents the residual curve after subtracting the theoretical peaks shown in (b). The dashed line indicates the residual curve after subtraction of the peak shapes due to the Cu-O(eq), Cu···C(eq), O(eq)···O(eq), and Cu···N(eq) interactions. The dotted line is finally obtained by subtraction of the caluclated peaks due to the Cu-O(ax) and O(eq)···O(ax) interactions. (b) and (c); The theoretical peak shapes of each atom-pair.

appear at about 400 pm, and the corresponding peak is in fact observed in the residual differential radial distribution curve.

Subtraction of peaks for the Cu–O(eq), Cu···C(eq), O(eq)···O(eq), and Cu···N(eq) interactions in the equatorial plane gives the residual curve (dashed line in Fig. 3a), in which a peak and a shoulder remain at 240 and 320 pm, respectively. The peak at 240 pm is thus ascribable to the Cu–O(ax) bonds within the distorted octahedral copper(II) ion. When the hexasolvated copper(II) ion has such a distorted octahedral structure, the interligand O(eq)···O(ax) interactions should cause a peak at about 320 pm. Since the areas under the peak at 240 pm and the shoulder at 320 pm correspond to two Cu–O bonds and approximately eight O(eq)···O(ax) interactions, respectively, we concluded that the solvated copper(II) ion in DMF has a distorted octahedral structure with six DMF molecules. Subtraction of the peaks due to the Cu–O(ax) and O(eq)···O(ax) interactions led to a smooth background curve (dotted line) having no appreciable peak remaining over the range $r<400$ pm.

The structural parameters for the $[\mathrm{Cu(dmf)_6}]^{2+}$ ion were refined by the least-squares method for the $s\cdot i(s)$ values over the range $s \geqslant 4\times10^{-2}$ pm^{-1} (Table 2). Structure parameters of atom-pairs within DMF molecules and perchlorate ions were quoted from the literature[5,9] and were fixed at the given values in the course of the calculation. The interatomic distances and temperature factors of interactions between copper(II) ion and atoms within DMF molecule were refined as independent variables as seen in the table (Column A). Lengths of interligand O(eq)···O(eq) and O(eq)···O(ax) interactions between DMF molecules coordinating to copper(II) ion were determined by the optimized Cu–O(eq) and Cu–O(ax) distances. Frequency factors of all interactions were kept constant during the calculation at the given values listed in the table which were evaluated on the basis of the distorted octahedral $[\mathrm{Cu(dmf)_6}]^{2+}$ structure model. The Cu–O(eq) and Cu–O(ax) distances within the $[\mathrm{Cu(dmf)_6}]^{2+}$ in DMF were finally determined to be 203 (3) and 243 (5) pm, respectively.

Table 2. Results of the Least-Squares Refinements of Solutions A to C. Standard Deviations Are Given in Parentheses

Interaction	Parameter	A	B	C
Cu–O(eq)	r/pm	203(3)	201(1)	201(1)
	b/10 pm^2	2(1)	1(1)	1(1)
	n	4[a]	4[a]	4[a]
Cu–O(ax)	r/pm	243(5)	246(4)	246(2)
	b/10 pm^2	3(1)	3(1)	4(1)
	n	2[a]	2[a]	2[a]
O(eq)···O(eq)	r[b]/pm	287	284	284
	b/10 pm^2	6[a]	6[a]	6[a]
	n	4[a]	4[a]	4[a]
O(eq)···O(ax)	r[c]/pm	317	318	317
	b/10 pm^2	12[a]	12[a]	12[a]
	n	8[a]	8[a]	8[a]
Cu···C(eq)	r/pm	289(5)	287(1)	287(1)
	b/10 pm^2	5(2)	5(1)	4(1)
	n	4[a]	4[a]	4[a]
Cu···O(eq) ($\mathrm{NO_3^-}$)	r/pm	—	370(5)	367(2)
	b/10 pm^2	—	12(4)	14(5)
	n	—	2[a]	2[a]
Cu···N(eq)	r/pm	404(9)	402(3)	402(2)
	b/10 pm^2	11(10)	10(4)	9(3)
	n	4[a]	3[a]	3[a]

a) The values were kept constant during the calculation. b) $r_{\mathrm{O(eq)\cdots O(eq)}}=\sqrt{2}\,r_{\mathrm{Cu-O(eq)}}$. c) $r_{\mathrm{O(eq)\cdots O(ax)}}=\sqrt{r_{\mathrm{Cu-O(eq)}}{}^2+r_{\mathrm{Cu-O(ax)}}{}^2}$.

The Cu–O(eq) bond length within the $[\mathrm{Cu(dmf)_6}]^{2+}$ complex in DMF is longer than that within the $[\mathrm{Cu(H_2O)_6}]^{2+}$ in aqueous solution (194—197 pm)[5,14] and that within the $[\mathrm{CuCl}_n(\mathrm{CH_3OH})_{6-n}]^{(2-n)+}$ (n=1—3) in methanolic solution (192.6—195.0 pm).[15] On the other hand, the Cu–O(ax) distance within the $[\mathrm{Cu(dmf)_6}]^{2+}$ ion is practically the same as that within the $[\mathrm{Cu(H_2O)_6}]^{2+}$.[5]

Copper(II) Nitrate DMF Solutions. Since concentrations of copper(II) ions in solutions B and C are much higher than the concentration in solution A, the structure analysis for the copper(II) ion in solutions B and C may give more reliable results than those obtained in solution A. However, a possibility of formation of contact ion pairs between copper(II) and nitrate ions should be taken into consideration in such concentrated solutions.

The $(D(r)-4\pi r^2\rho_0)$ curve of solution B depicted in Fig. 4a was analyzed by the similar way to that employed for solution A. We first assumed that the copper(II) ion in solution B has the same structure as that in solution A. Subtraction of theoretical peaks originating from the intramolecular interactions of DMF molecules and nitrate ions gave the chain line in Fig. 4a. Further subtraction of peaks arising from the Cu–dmf(eq) interactions, i.e., the Cu–O(eq), Cu···C(eq), O(eq)···O(eq), and Cu···N(eq), led to the residual curve expressed by the dashed line. In the curve we see a distinct peak at 245 pm and very broad humps around 320 and 370 pm. The peak at 245 pm is easily attributable to the Cu–O(ax) bond. Therefore, the first hump around 320 pm may be ascribable to the O(eq)···O(ax) interaction as also found in solution A. The broad hump around 370 pm has not been observed in solution A and thus it might be the one characteristic of metal nitrate DMF solutions. Such a broad peak has been observed in the radial distribution curve of nickel(II) nitrate DMF solution,[16] but not in DMF solutions of the perchlorate.[17] Accordingly, the peak is expected to be due to interactions between copper(II) ion and atoms within nitrate ion.[18]

Nitrate ion can coordinate to copper(II) ion as

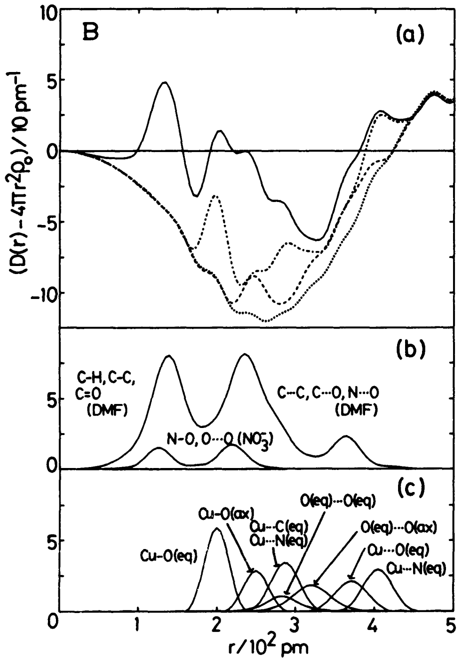

Fig. 4. (a); The $(D(r)-4\pi r^2\rho_o)$ curve for solution B. The chain line represents the residual curve after subtracting the theoretical peaks shown in (b). The dashed line indicates the residual curve after subtraction of the peak shapes due to the Cu-O(eq), Cu···C(eq), O(eq)···O(eq), and Cu···N(eq) interactions. The dotted line is finally obtained by subtraction of the calculated peaks due to the Cu-O(ax), O(eq)···O(ax), and Cu···O(eq) interactions. (b) and (c); The theoretical peak shapes of each atom pair.

either mono- or bidentate ligand. However, the broad peak at 370 pm observed could not be reproduced by a model that two oxygen atoms of a nitrate ion bind to copper(II) ion at the distance of 200 pm as a bidentate ligand. Therefore, it is suggested that a nitrate ion binds to copper(II) ion at the equatorial position to form $[CuNO_3(dmf)_5]^+$. In order to reproduce the peak at 370 pm, we examined various configurations of nitrate ion within the $[CuNO_3(dmf)_5]^+$ complex. The most plausible binding mode of a nitrate ion to the copper(II) ion is that a nitrate ion directs one oxygen atom toward the copper(II) ion with the Cu-O-N angle of ca. 120° in the equatorial plane of the copper(II) ion and the triangular plane of the nitrate ion is perpendicular to the square-plane within the complex. According to the model, the broad peak at 370 pm is due to two nonbonding $Cu\cdots O(NO_3^-)$ interactions. In fact, the area under the hump corresponds to two Cu···O interactions.

The $(D(r)\text{-}4\pi r^2\rho_o)$ curve for solution C was also well explained in terms of the formation of the $[CuNO_3(dmf)_5]^+$ complex having the distorted octahedral structure as has been seen in solution B.

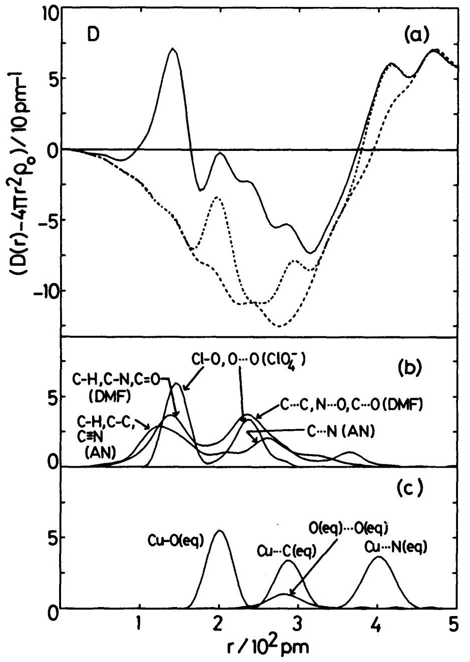

Fig. 5. (a); The $(D(r)-4\pi r^2\rho_o)$ curve for solution D. The chain line represents the residual curve after subtracting the theoretical peaks shown in (b). The dashed line indicates the residual curve after subtraction of the peak shapes due to the Cu-O(eq), Cu···C(eq), O(eq)···O(eq), and Cu···N(eq) interactions shown in (c). (b) and (c); The theoretical peak shapes of each atom pair.

The structure parameters for the $[CuNO_3(dmf)_5]^+$ in solutions B and C were optimized by least-squares calculations by using the data in the high-angle region of $s\cdot i(s)$ ($s \gg 4\times10^{-2}\,pm^{-1}$) and the results are summarized in Table 2 (Columns B and C). Very similar results are obtained for both solutions. In the course of the calculation the $Cu\cdots N(NO_3^-)$ interaction was regarded as one of the four Cu···C(eq) interactions, since nitrogen atom is practically indistinguishable from carbon atom by the X-ray diffraction method and no significant error could be introduced by this simplification. Other assumptions adopted for the refinements are the same as those for solution A. The Cu-O(eq) and Cu-O(ax) bond lengths thus optimized are 201 (1) and 246 (4) pm, respectively.

Copper(II) Perchlorate DMF-AN Solutions. From the stability constants reported for copper(II)-dmf complexes in AN,[3] both $[Cu(dmf)_4]^{2+}$ and $[Cu(dmf)_6]^{2+}$ ions are expected to exist in solutions D and E.

The solid and chain lines in Fig. 5a represent the observed $(D(r)-4\pi r^2\rho_o)$ curve for solution D and the residual curve after subtraction of peaks due to the atom pairs within DMF, AN and perchlorate indicated in Fig. 5b from the original one, respectively. In the residual curve three peaks appear around 200, 290, and 400 pm as seen in solutions A to C, which can be assigned to the Cu–O, Cu···C, and Cu···N interactions, respectively, in the equatorial plane, because the shape analysis of the peak at 200 pm gave the coordination number of four for the Cu–O bonds. On the other hand, no clear indication was obtained for the Cu–X(ax) bonds, where X denotes either oxygen atom within DMF or nitrogen atom within AN, over the region $r<300$ pm in contrast to the case of solutions A to C. Subtraction of peaks due to the Cu–O(eq), Cu···C(eq), O(eq)···O(eq), and Cu···N(eq) interactions led to the residual curve (dashed line in Fig. 5a), in which a small peak appearing at about 250 pm suggests that a part of copper(II) ions might have some interactions with the solvent molecules along the axis of copper(II) ion, but it is obvious that this peak is too small to conclude that all of copper(II) ions have the six-coordination structure as have been seen in solutions A to C.

The average scattering density ρ_0 in a stoichiometric volume of solution D (1.993×10^{-4} pm^{-3}) is very close to the ρ_0 value of solution B (1.934×10^{-4} pm^{-3}), and hence the background curves for both solutions should have the same feature. Therefore, the residual curve drawn by the dashed line in Fig. 5a, in which the Cu–X(ax) bonds were not taken into account, should overlap the one represented by the dotted line in Fig. 4a, which was obtained by taking the Cu–O(ax) bonds into consideration, in the region of $r<300$ pm. The two curves sufficiently fit each other and thus copper(II) ion in solution D is practically not solvated at the axial position within 300 pm.

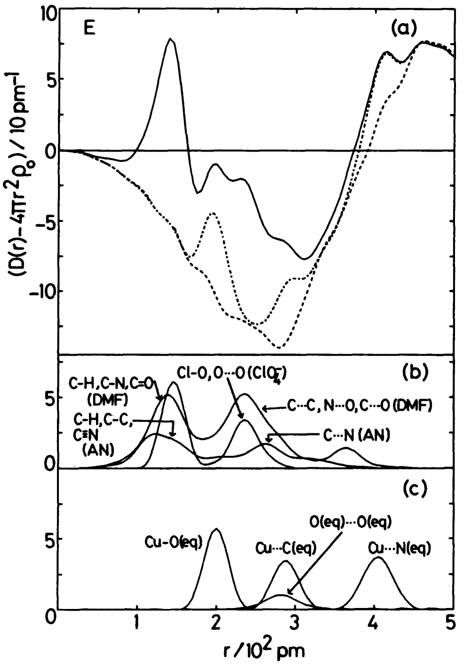

Fig. 6. (a); The ($D(r)-4\pi r^2\rho_0$) curve for solution E. The chain line represents the residual curve after subtracting the theoretical peaks shown in (b). The dashed line indicates the residual curve after subtraction of the peak shapes due to the Cu–O(eq), Cu···C(eq), O(eq)···O(eq), and Cu···N(eq) interactions shown in (c). (b) and (c); The theoretical peak shapes of each atom pair.

Analysis of the ($D(r)-4\pi r^2\rho_0$) curve shown in Fig. 6a for solution E, in which the concentration of DMF is higher than that in solution D, gave the similar result to that obtained for solution D. In the residual curve (dashed line) after subtraction of the peak shapes due to the intramolecular structure of DMF, AN and perchlorate and due to the Cu–O(eq), Cu···C(eq), O(eq)···O(eq), and Cu···N(eq) interactions, no distinct peak to be assignable to the Cu–X(ax) bonds was observed over the range $r<300$ pm. The X-ray scattering data for solution E colud be well reproduced by the same structural model as that for solution D and, therefore, we concluded that most of the solvated copper(II) ion in solutions D and E has the square-planar structure and solvent molecules do practically not coordinate to the copper(II) ion along the axis through the square-plane.

The structure parameters for the $[\mathrm{Cu(dmf)_4}]^{2+}$ ion in DMF–AN mixtures were finally determined by least-squares calculations. The least-squares method was applied to the $s\cdot i(s)$ curve over the range $s\geqslant4\times10^{-2}$ pm^{-1} by using similar assumptions to those adopted for solutions A to C. The results obtained are listed in Table 3. The Cu–O(eq) distance is 200 (1) pm and practically the same as that within the $[\mathrm{Cu(dmf)_6}]^{2+}$ ion in DMF.

In a previous calorimetric investigation of dilute solution of copper(II) ions in DMF–AN mixtures, formation of the $[\mathrm{Cu(dmf)_6}]^{2+}$ complex is proposed in AN containing a large excess of DMF (ca. 1 mol dm^{-3}) compared with copper(II) ions.[3] In

Table 3. Results of the Least-Squares Refinements of Solutions D and E. Standard Deviations Are Given in Parentheses

Interaction	Parameter	D	E
Cu–O(eq)	r/pm	200(1)	199(1)
	b/10 pm^2	2(1)	1(1)
	n	4$^{a)}$	4$^{a)}$
O(eq)···O(eq)	$r^{b)}$/pm	282	282
	b/10 pm^2	6$^{a)}$	6$^{a)}$
	n	4$^{a)}$	4$^{a)}$
Cu···C(eq)	r/pm	285(2)	288(1)
	b/10 pm^2	5(2)	5(1)
	n	4$^{a)}$	4$^{a)}$
Cu···N(eq)	r/pm	399(3)	402(2)
	b/10 pm^2	15(5)	13(3)
	n	4$^{a)}$	4$^{a)}$

a) The values were kept constant during the calculation. b) $r_{\mathrm{O(eq)\cdots O(eq)}}=\sqrt{2}\,r_{\mathrm{Cu-O(eq)}}$.

DMF-AN mixtures of concentrated copper(II) perchlorate solutions which have relatively low $C_{\mathrm{dmf}}/C_{\mathrm{Cu}}$ values of 5—7 examined in this study, the concentration of free DMF may not be sufficiently high to establish the equilibrium completely to the right-hand side

$$[\mathrm{Cu(dmf)_4}]^{2+} + 2\mathrm{dmf} \rightleftharpoons [\mathrm{Cu(dmf)_6}]^{2+}$$

by forming the weak Cu-O(ax) bonds. Interactions between DMF and AN[19,20] may lower the activity of free DMF in the bulk of the mixture so as to prevent establishment of the equilibrium. Acetonitrile solvates copper(II) ion much more weakly than DMF does, and thus copper(II) ions in solutions D and E mainly exist as the square-planar $[\mathrm{Cu(dmf)_4}]^{2+}$ species.

The work has been financially supported by the Grant-in-Aid for Special Project Research No. 61134043 from the Ministry of Education, Science and Calture. Computer calculations were carried out at the computer center of the Institute for Molecular Science in Okazaki.

References

1) S. Ishiguro, B. G. Jeliazkova, and H. Ohtaki, *Bull. Chem. Soc. Jpn.*, **58**, 1143 (1985).

2) S. Ishiguro, B. G. Jeliazkova, and H. Ohtaki, *Bull. Chem. Soc. Jpn.*, **58**, 1749 (1985).

3) S. Ishiguro, B. G. Jeliazkova, and H. Ohtaki, *J. Solution Chem.*, **16**, 1 (1987).

4) S. Ishiguro, B. G. Jeliazkova, and H. Ohtaki, *Bull. Chem. Soc. Jpn.*, **59**, 1073 (1986).

5) H. Ohtaki and M. Maeda, *Bull. Chem. Soc. Jpn.*, **47**, 2197 (1974).

6) H. Ohtaki, *Rev. Inorg. Chem.*, **4**, 103 (1982).

7) G. Johansson and M. Sandström, *Chem. Scr.*, **4**, 195 (1973).

8) T. Yamaguchi, Doctor Thesis, Tokyo Institute of Technology, 1978.

9) H. Ohtaki, S. Itoh, T. Yamaguchi, S. Ishiguro, and B. M. Rode, *Bull. Chem. Soc. Jpn.*, **56**, 3406 (1983).

10) A. Kratochwill, J. U. Weidner, and H. Zimmermann, *Ber. Bunsenges. Phys. Chem.*, **77**, 408 (1973).

11) H. Bertagnolli, P. Chieux, and M. D. Zeidler, *Mol. Phys.*, **32**, 759, 1731 (1976).

12) R. Caminiti, G. Licheri, G. Piccaluga, and G. Pinna, *J. Chem. Phys.*, **68**, 1967 (1978).

13) L. B. Brun and C.-I. Brändên, *Acta Crystallogr.*, **20**, 749 (1966).

14) M. Magini, *Inorg. Chem.*, **21**, 1535 (1982).

15) M. Ichihashi, H. Wakita, and I. Masuda, *Bull. Chem. Soc. Jpn.*, **56**, 3761 (1983).

16) K. Ozutsumi, S. Ishiguro, and H. Ohtaki, unpublished data.

17) K. Ozutsumi, T. Takamuku, S. Ishiguro, and H. Ohtaki, to be published.

18) An electronic spectrum for solution B shows a larger absorption maxima (ε=600 dm^2 mol^{-1} at λ=797 nm) than that for solution A (ε=260 dm^2 mol^{-1} at λ=790 nm), suggesting the coordination of nitrate ion to copper(II) ion.

19) I. Katime and L. C. Cesteros, *J. Chem. Soc., Faraday Trans. 2*, **80**, 1215 (1984).

20) A. K. Sharman, D. R. Sharman, and D. S. Gill, *J. Phys. D*, **18**, 1199 (1985).